Supporting Information for:

Biogas upgrading through kinetic separation of carbon dioxide and methane over Rb- and Cs-ZK-5 zeolites

Tom Remy,[a] Elena Gobechiya,[b] David Danaci,[c] Sunil A. Peter,[a] Penny Xiao,[c] Leen Van Tendeloo,[b] Sarah Couck,[a] Jin Shang,[c] Christine E.A. Kirschhock,[b] Ranjeet K. Singh,[c] Johan A. Martens,[b] Gino V. Baron,[a] Paul A. Webley,[c] and Joeri F.M. Denayer[a]*

[a] Department of Chemical Engineering, Vrije Universiteit Brussel, Pleinlaan 2, 1050 Brussels, Belgium

[b] Centre for Surface Chemistry and Catalysis, KU Leuven, Kasteelpark Arenberg 23, 3001 Leuven, Belgium

[c] Department of Chemical and Biomolecular Engineering, The University of Melbourne, 3010 Victoria, Australia

* Corresponding Author: Joeri F. M. Denayer

E-mail: joeri.denayer@vub.ac.be

Tel.: 02 629 17 98

Fax: 02 629 32 48

Table of contents

S1 Detailed synthesis procedure of K-ZK-5

The synthesis was based on the procedure as disclosed by Verduijn et al.[1] The synthesis system is SiO_2 - Al_2O_3 - KOH - $Sr(NO_3)_2$ - H_2O with the following molar composition 5 SiO_2 - Al_2O_3 - 2.3 KOH - 0.05 $Sr(NO_3)_2$ - 78 H_2O.

First, 4.5g H_2O (Milli-Q) are added to a polypropylene bottle (Nalgene, 100 mL) with 2.684g KOH (VWR, 85.9%) and 1.62g $Al(OH)_3$ (residue at 1373 K: 62 - 67%, BDH Chemicals Ltd.). This unclosed bottle is heated, while stirring, for about 20 min in an oil bath at 378 K until complete dissolution of $Al(OH)_3$. Afterwards, the bottle is weighed in order to determine the mass loss due to water evaporation during the heating.

In a second polypropylene bottle (Nalgene, 100 mL), 10.668g H_2O (Milli-Q) plus the amount lost of water during the heating is added to 15.634g Ludox HS-40 (Sigma-Aldrich, 40 wt% suspension in H_2O) under stirring.

A third polypropylene bottle (Nalgene, 100 mL) is used to mix 4.5 mL H_2O (Milli-Q) with 0.050g $Sr(NO_3)_2$ (VWR, 98 %) under stirring.

Afterwards, the content of the third polypropylene bottle is added drop by drop to the second one. Subsequently the mixture in the second bottle is added drop by drop to the first polypropylene bottle.

The resulting gel is transferred to a Teflon liner, put in an autoclave, and kept in a hot air oven at 423 K for at least 96 h. Finally the sample was vacuum-filtered and washed several times with deionized water and dried overnight at 353 K. With this procedure about 1.0 - 1.5g K-ZK-5 can be obtained per Teflon liner.

S2 Parameter calculation/estimation for breakthrough simulations

Conservation equations

The axial dispersion coefficients for CO_2 and CH_4 were calculated from the Wakao et al. correlation:[2]

$$D_{ax,i} = \frac{D_{m,i}}{\varepsilon_B} \cdot \left(E_0 + 0.5 \cdot \mathrm{Re} \cdot Sc\right)$$

The Reynolds (Re) and Schmidt (Sc) numbers for CO_2 and CH_4 were calculated as follows:

$$\mathrm{Re} = \left.\frac{\rho_g \cdot v \cdot d_p}{\mu_g}\right|_{in}$$

$$Sc = \left.\frac{\mu_g}{\rho_g \cdot D_m}\right|_{in}$$

E_0 represents the stagnant contribution to the axial dispersion and a value of 0.23 has been recommended.[3] The temperature dependence of the molecular diffusion coefficient is given by:[3]

$$D_{m,i}\big|_T = D_{m,i}\big|_{T_{ref}} \cdot \left(\frac{T}{T_{ref}}\right)^{1.75}$$

Molecular diffusion coefficients at a reference temperature of 293 K were taken from Delgado et al.[3] The obtained axial dispersion coefficients for CO_2 and CH_4 are 7.1 x 10^{-5} m^2/s and 7.7x 10^{-5} m^2/s respectively.

The pellet density is calculated from the following equation[4]:

$$\rho_p = (1 - \varepsilon_p) \cdot \rho_c$$

The crystal density ρ_c can be estimated from framework density (given on the IZA website) and mass of unit cell, whose composition has been determined by ICP.

For the simulations, the following typical values for ε_p and ε_B were used:

$\varepsilon_p = 0.5$

$\varepsilon_B = 0.4$

This results in a typical value of 0.7 for the total porosity, where the total porosity was calculated via[4]:

$$\varepsilon_t = \varepsilon_B + (1 - \varepsilon_B) \cdot \varepsilon_p$$

Momentum balance - Ergun equation

The density of the gas mixture is obtained from:[5]

$$\rho_g = \frac{\left(\sum_j y_j \cdot MW_j\right) \cdot P}{R_g \cdot T}$$

The viscosity of the gas mixture is obtained from the Wilke equation:[6]

$$\mu_g = \mu_{mix} = \sum_i \frac{\mu_i \cdot y_i}{\sum_j y_j \cdot \Phi_{ij}}$$

in which:

$$\Phi_{ij} = \mu_{mix} = \frac{\left(1 + \sqrt{\frac{\mu_i}{\mu_i}} \cdot \left(\frac{MW_j}{MW_i}\right)^{1/4}\right)^2}{\sqrt{8 \cdot \left(1 + \frac{MW_i}{MW_j}\right)}}$$

This function is dimensionless and equal to 1 when i = j.

The pure component viscosities are calculated from the Chapmann-Enskog equation:[6]

$$\mu_g = 26.69 \cdot 10^{-7} \cdot \frac{\sqrt{MW_i \cdot T}}{\sigma_c^2 \cdot \Omega_\mu}$$

Pure component values for σ_c and Ω_μ can be found in book of Bird et al[6].

Boundary conditions

The boundary conditions consist of the well-known Danckwertz boundary conditions[4]:

$$\left[v \cdot C_i\right]\Big|_{in} = \left[v \cdot C_i\right]\Big|_{z=0} - D_{ax,i} \cdot \left.\frac{\partial C_i}{dz}\right|_{z=0}$$

$$\left.\frac{\partial C_i}{dz}\right|_{z=L} = 0$$

In addition, the exit pressure of the bed is fixed at 1 bar or any pressure given as setpoint to the backpressure regulator.

S3 PSA Simulations

For comparative purposes a simple 6-step PSA process with 2 beds for separation of an equimolar CO_2/CH_4 mixture was used (Figure S1). The separation consists of the following steps: feed (bed 1) via vacuum evacuation (bed 2) (step 1)- pressure equalization via the product ends between bed 1 and bed 2 (step 2) - depressurization (bed 1) via repressurization with feed (bed 2) (steps 3 + 4) - pressure equalization via the product ends between bed 1 and bed 2 (step 5) - repressurization with feed (bed 1) via depressurization of bed 2 (step 6).

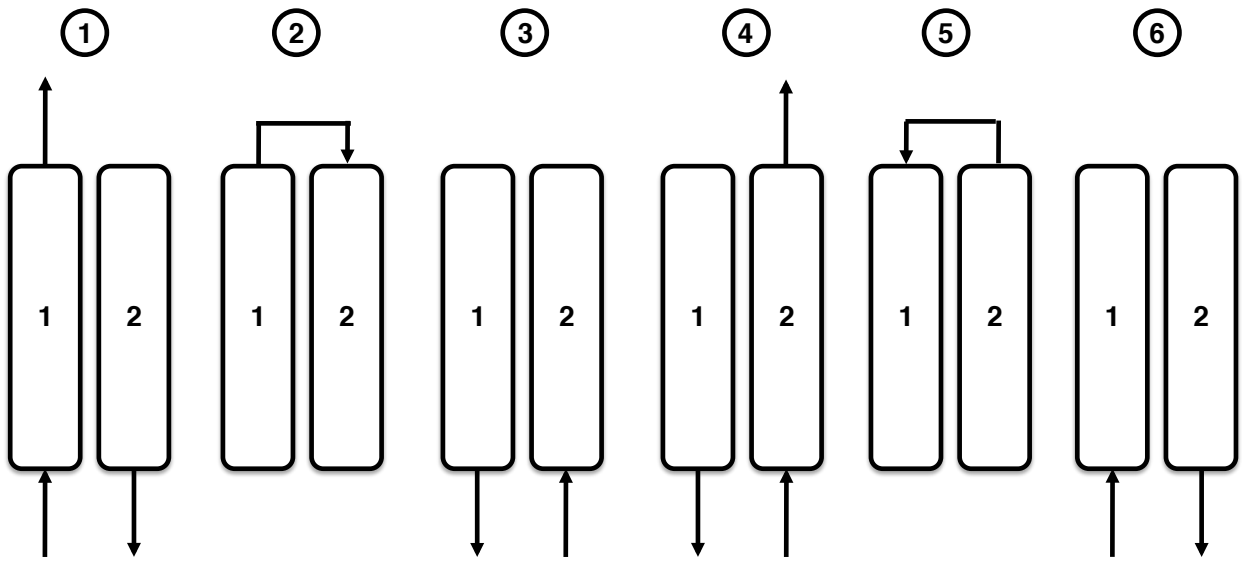

Figure S1. Six-step PSA process for separation of an equimolar CO_2/CH_4 mixture.

The function of each step for bed 1 in the context of CO_2/CH_4 separation is briefly explained below:[4, 7]

1. Feed with raffinate withdrawal

   Withdrawal of raffinate at high purity (CH_4 production step). In a PSA process, the raffinate is by definition the weakest adsorbed component (CH_4 in this case). The feed gas containing 40% CO_2 balanced with CH_4 enters the system at high pressure. CO_2 is adsorbed and highly pure CH_4 (CH4 product) exits from the bed.

2. Pressure equalization

   After the second bed completed the evacuation step and the first the feed step, both beds are connected via their product ends until the pressures in both beds get equal. Since the second bed is now partly pressurized with gas from the first bed, energy is being conserved. At the same time, separative work is conserved as the stream from bed 1 to bed 2 is depleted in the strongly adsorbed component (CO_2). This step will benefit a high CO_2 concentration product in the next steps.

3. Depressurization

   Achieving high purity of both extract and raffinate products. This is the preferred regeneration option when the extract (CO_2) is strongly adsorbed. In a PSA process, the extract is by definition the strongest adsorbed component (CO_2 in this case). As the pressure in the bed is released, the adsorbed CO_2 adsorbed is released into the gas phase at a low pressure.

4. Evacuation (vacuum regeneration)

Same as for step 3, with concurrent raffinate withdrawal from bed 2. Because CO_2 is strongly adsorbed, a very low pressure is required to remove CO_2 from the bed using a vacuum pump.

5. Pressure equalization

   See step 2, but now beds 1 and 2 are interchanged.

6. Repressurization

   Enrichment of the less adsorbed species (CH_4) in the gas phase at the product end (production of CH_4 with high purity). The bed is repressurized with feed gas until the pressure reaches that in step 1.

As a result, pure CH_4 (raffinate) and high concentration CO_2 (extract) can be generated continuously with the cyclic process.

The parameters for the reference PSA process are given in Table S1 - S2.

Table S1. Parameters for PSA separation of CO_2/CH_4 mixtures.

Parameter	Value
ε_B (-)	0.37
ε_p (-)	0.6
ρ_p (kg/m^3)	641
d_p (m)	0.002
C_p (J/(kg.K))	1000
Wall thickness (m)	3.5×10^{-3}
C_{pW} (J/(kg.K))	477
ρ_W (kg/m^3)	7900
Bed length (m)	1.0
Bed internal diameter (m)	1×10^{-2}
$T_{ambient}$ (K)	303.15
$P_{ambient}$ (bar)	1.01325
$T_{initial}$ (K)	303.15
$P_{initial}$ (bar)	2.0
$y_{CO2initial}$	0.5
$y_{CH4initial}$	0.5

For comparative purposes, the same value for the bed porosity, pellet porosity, adsorbent density, pellet diameter and adsorbent heat capacity were assigned to each adsorbent. Mixture properties were calculated in the same way as for the breakthrough simulations (see section S1).

Table S2. Step times and pressures at the end of each step for PSA separation of an equimolar CO_2/CH_4 mixture on different adsorbents (PE = pressure equalization, depres. = depressurization, ev. = evacuation, repres. = repressurization).

13X					
F_{in} = 1.485 mol/s (2 Nl/min)					
t_{feed} = 55s	t_{PE1} = 5s	$t_{depres.}$ = 50s	$t_{ev.}$ = 55s	t_{PE2} = 5s	$t_{repres.}$ = 50s
P_{feed} = 2 bar	P_{PE1} = 0.92 bar	$P_{depres.}$ = 0.15 bar	$P_{ev.}$ = 0.10 bar	P_{PE2} = 0.9 bar	$P_{repres.}$ = 2.02 bar
Rb-ZK-5					
F_{in} = 5.0 x 10^{-4} mol/s (0.67 Nl/min)					
t_{feed} = 30s	t_{PE1} = 5s	$t_{depres.}$ = 100s	$t_{ev.}$ = 30s	t_{PE2} = 5s	$t_{repres.}$ = 100s
P_{feed} = 2 bar	P_{PE1} = 1.05 bar	$P_{depres.}$ = 0.1 bar	$P_{ev.}$ = 0.1 bar	P_{PE2} = 1.05 bar	$P_{repres.}$ = 2.02 bar
Cs-ZK-5					
F_{in} = 2.0 x 10^{-4} mol/s (0.67 Nl/min)					
t_{feed} = 25s	t_{PE1} = 5s	$t_{depres.}$ = 100s	$t_{ev.}$ = 25s	t_{PE2} = 5s	$t_{repres.}$ = 100s
P_{feed} = 2 bar	P_{PE1} = 1.0 bar	$P_{depres.}$ = 0.05 bar	$P_{ev.}$ = 0.05 bar	P_{PE2} = 1.0 bar	$P_{repres.}$ = 2.02 bar

S4 XRD patterns

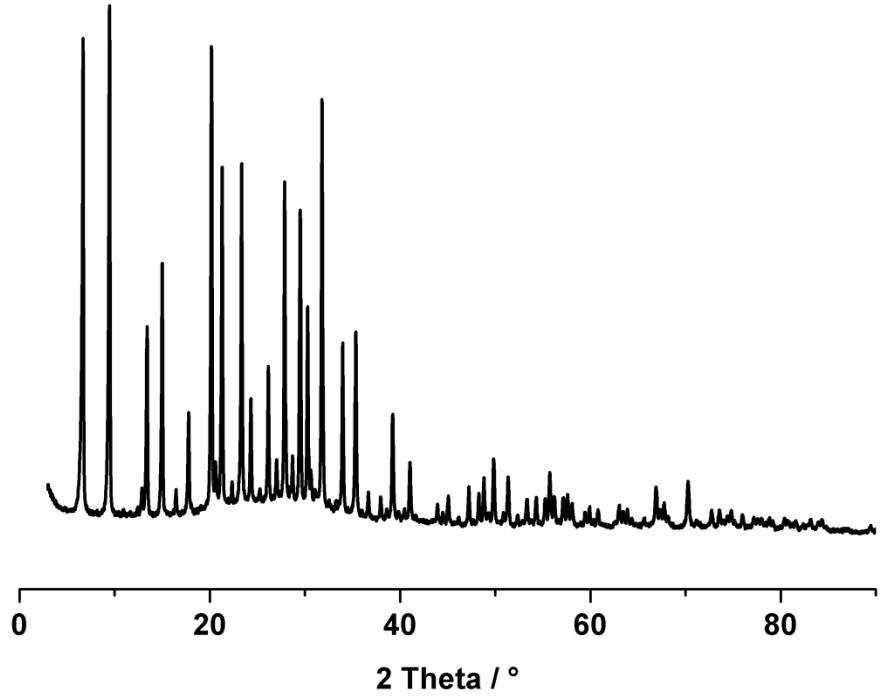

Figure S2. XRD pattern of Rb-ZK-5.

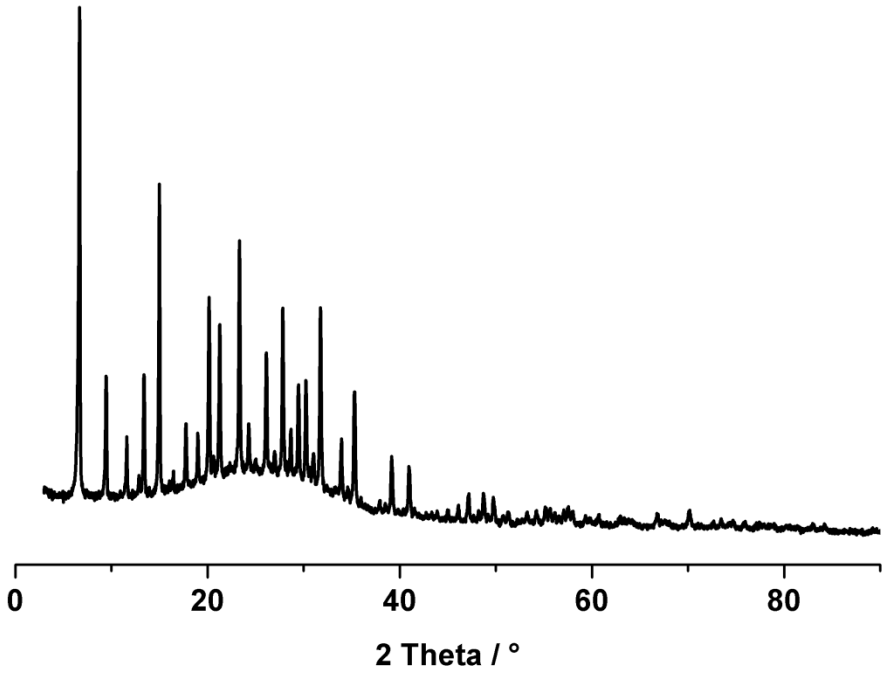

Figure S3. XRD pattern of Cs-ZK-5.

S5 SEM results

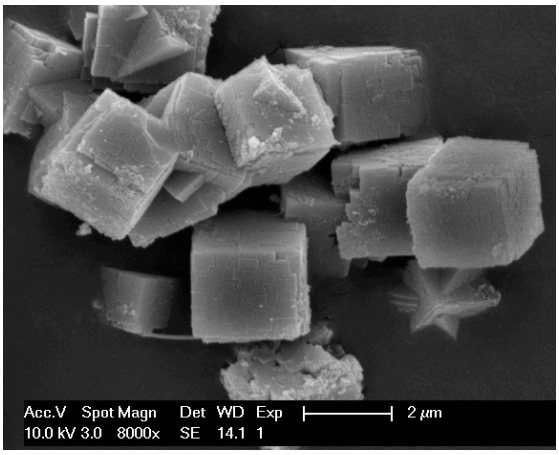

Figure S4. SEM image from as-synthesized K-ZK-5.

S6 Rietveld refinements

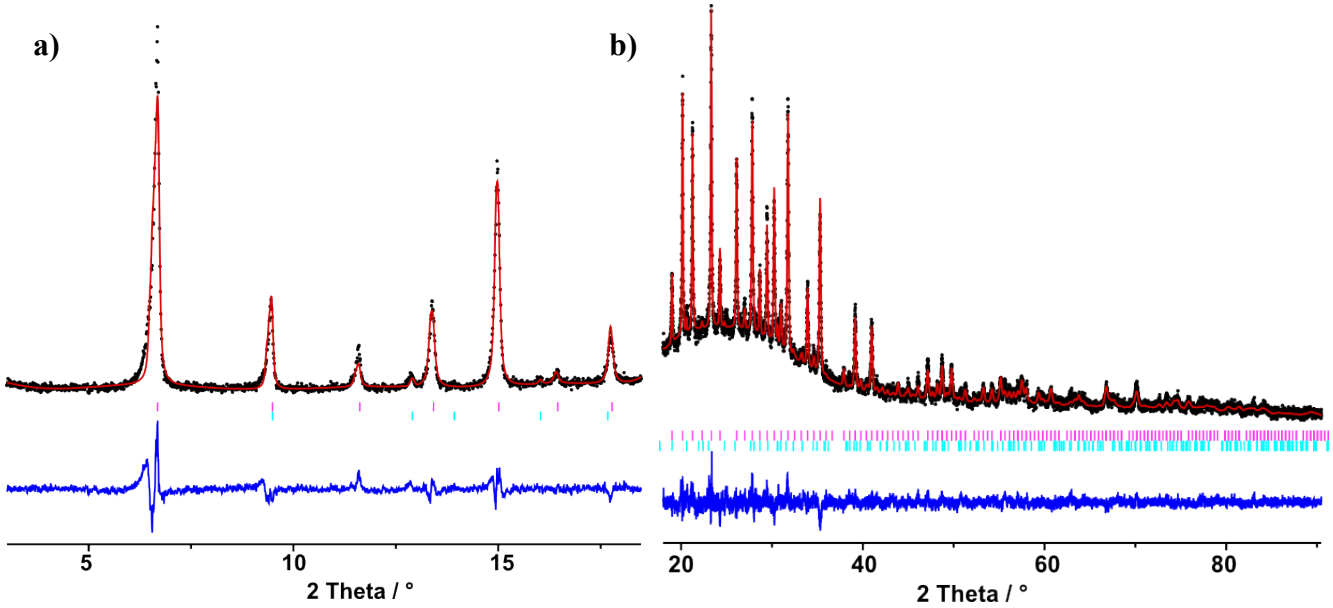

Figure S5. Rietveld plots for the XRD profile of Cs-ZK-5; R_{wp} = 5.51, R_p = 4.21%, χ^2 = 1.40; observed (black dots) and calculated (red solid line) patterns, the difference plot (blue bottom curve) and positions for Bragg-reflections (purple vertical bars - Cs-ZK-5; light blue vertical bars - chabazite): a) low-angle region; R_F2 = 4.43%; b) high-angle region; R_F2 = 14.80%.

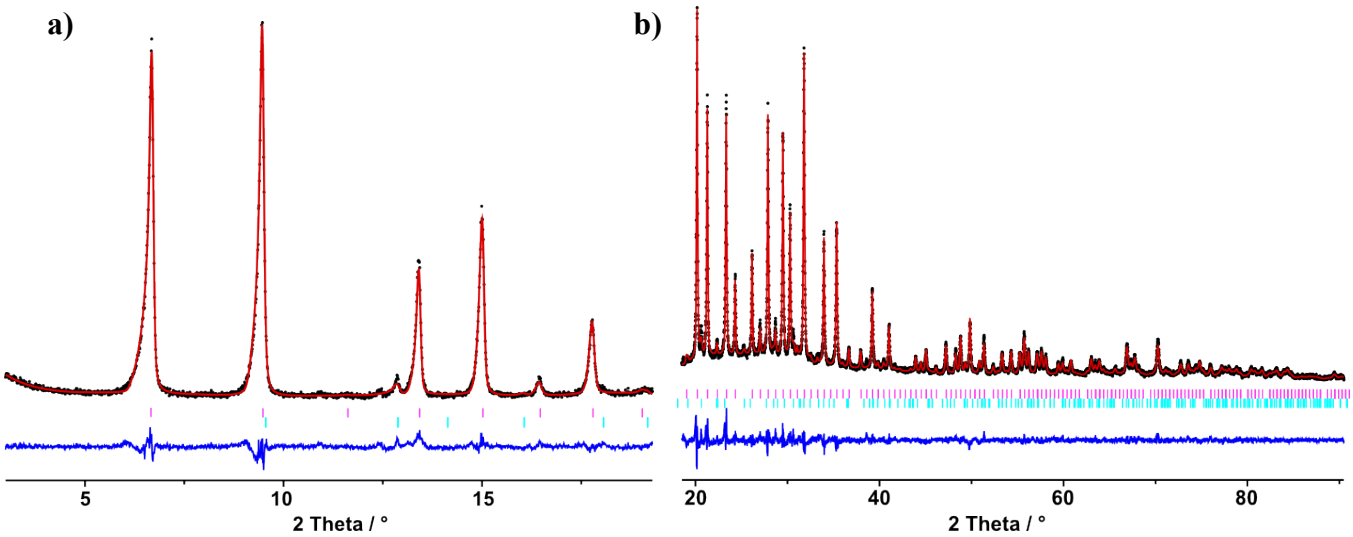

Figure S6. Rietveld plots for the XRD profile of Rb-ZK-5; R_{wp} = 5.99, R_p = 4.72%, χ^2 = 1.59; observed (black dots) and calculated (red solid line) patterns, the difference plot (blue bottom curve) and positions for Bragg-reflections (purple vertical bars - Rb-ZK-5; light blue vertical bars - chabazite): a) low-angle region; R_F2 = 3.90%; b) high-angle region; R_F2 = 12.17%.

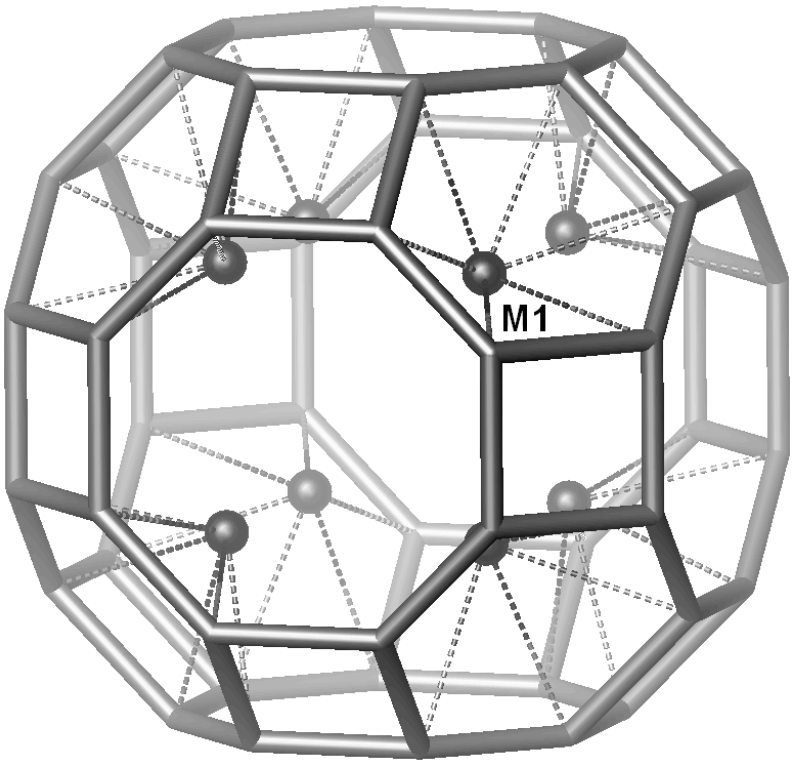

Figure S7. Location of the M1-site within Rb-ZK-5.

S7 Dual-site Langmuir fits

Table S3. Dual-site Langmuir constants for CO_2 and CH_4 on Rb-ZK-5 and Cs-ZK-5

Rb-ZK-5		
	CO_2	**CH_4**
q_{1sat} (mol/kg)	2.08 ± 0.11	1.43 ± 0.04
q_{2sat} (mol/kg)	2.28 ± 0.11	21 ± 16
b_{10} (1/kPa)	$(3.0 \pm 2.9) \times 10^{-11}$	$(6.3 \pm 3.1) \times 10^{-5}$
Q_1 (J/mol)	$(46.4 \pm 2.5) \times 10^{3}$	$(11.1 \pm 1.2) \times 10^{3}$
b_{20} (1/kPa)	$(7.19 \pm 0.14) \times 10^{-11}$	$(3.1 \pm 1.5) \times 10^{-24}$
Q_2 (J/mol)	$(54.7 \pm 5.1) \times 10^{3}$	$(102.0 \pm 0.3) \times 10^{3}$
b_1 @ 298 K (1/kPa)	4.0×10^{-3}	5.5×10^{-3}
b_2 @ 298 K (1/kPa)	0.28	2.3×10^{-6}
Cs-ZK-5		
	CO_2	**CH_4**
q_{1sat} (mol/kg)	2.55 ± 0.27	3.6 ± 6.2
q_{2sat} (mol/kg)	2.16 ± 0.09	1.26 ± 0.22
b_{10} (1/kPa)	$(6.4 \pm 3.7) \times 10^{-7}$	$(8.56 \pm 0.18) \times 10^{-8}$
Q_1 (J/mol)	$(18.8 \pm 1.6) \times 10^{3}$	$(18.2 \pm 2.5) \times 10^{3}$
b_{20} (1/kPa)	$(1.9 \pm 2.3) \times 10^{-8}$	$(1.32 \pm 0.92) \times 10^{-6}$
Q_2 (J/mol)	$(38.9 \pm 3.3) \times 10^{3}$	$(21.2 \pm 2.0) \times 10^{3}$
b_1 @ 298 K (1/kPa)	1.3×10^{-3}	1.3×10^{-4}
b_2 @ 298 K (1/kPa)	0.12	6.9×10^{-3}

S8 Breakthrough data

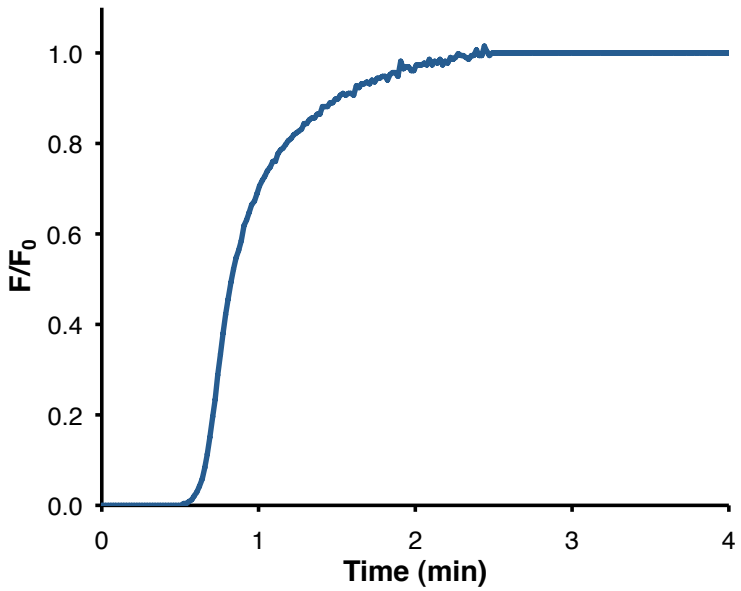

Figure S8. Pure CH_4 breakthrough profile on Rb-ZK-5 at 308 K and 1 bar (F_{TOT} = 10 NmL/min).

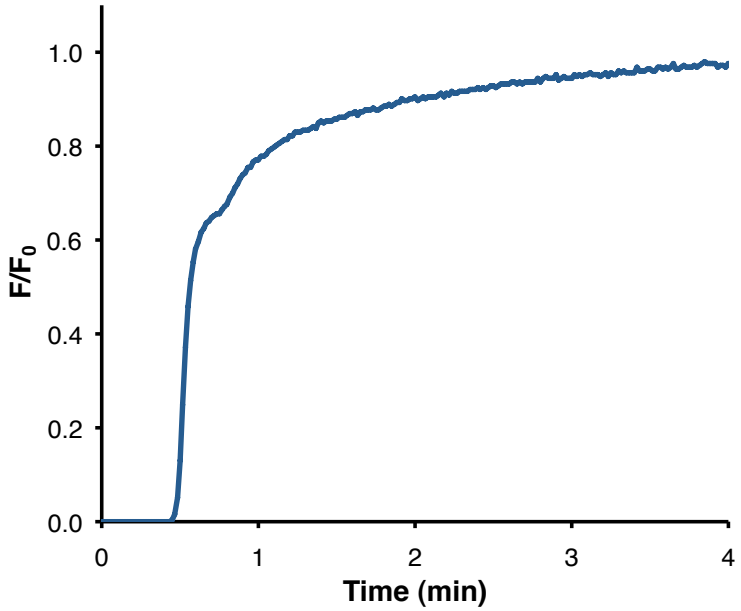

Figure S9. Pure CH_4 breakthrough profile on Cs-ZK-5 at 308 K and 1 bar (F_{TOT} = 10 NmL/min).

S9 Notation

b = Henry constant (kPa^{-1})

b_0 = Henry pre-exponential factor (kPa^{-1})

C = concentration (mol/m^3)

C_p = pellet heat capacity (J/kg/K)

C_{pW} = wall heat capacity (J/kg/K)

D_{ax} = axial dispersion coefficient (m^2/s)

D_m = molecular diffusion coefficient (m^2/s)

d_p = particle diameter (m)

E_0 = stagnant contribution to axial disperison (-)

F = flow rate (Nl/min or Nml/min)

L = column length (m)

MW = molecular weight (kg/kmol)

Re = Reynolds number (-)

P = pressure (Pa)

R_g = gas constant (J/mol/K)

Q = Langmuir adsorption heat (J/mol)

q_{sat} = saturation loading (mol/kg)

Sc= Schmidt number (-)

T = temperature (K)

v = interficial velocity (m/s)

y = mole fraction (-)

z = axial position (m)

ε_B = bed porosity (-)

ε_p = pellet porosity (-)

ε_t = total porosity (-)

σ_c = collision diameter (Å)

Ω_{μ} = collision integral

ρ_c = crystal density (kg/m^3)

ρ_g = gas density (kg/m^3)

ρ_p = pellet density (kg/m^3)

ρ_W = wall density (kg/m^3)

μ_g = gas viscosity (Pa.s)

S10 References

1. *U.S. Pat.*, 4,994,249, 1991.
2. N. Wakao, S. Kaguei and H. Nagai, *Chem. Eng. Sci.*, 1978, **33**, 183-187.
3. J. A. Delgado, M. A. Uguina, J. L. Sotelo, B. Ruiz and J. M. Gomez, *Adsorption*, 2006, **12**, 5-18.
4. D. M. Ruthven, S. Farooq and K. S. Knaebel, in *Pressure Swing Adsorption*, VCH Publishers, Inc., New York, 1994.
5. R. S. Todd, G. B. Ferraris, D. Manca and P. A. Webley, *Comput. Chem. Eng.*, 2003, **27**, 883-899.
6. R. B. Bird, W. E. Stewart and E. N. Lightfoot, in *Transport Phenomena*, John Wiley & Sons, Inc. , New York, 1960.
7. C. A. Grande and A. E. Rodrigues, *Ind. Eng. Chem. Res.*, 2007, **46**, 4595-4605.